nature ecology & evolution

ARTICLES

DOI: 10.1038/s41559-017-0301-9

Ichnological evidence for meiofaunal bilaterians from the terminal Ediacaran and earliest Cambrian of Brazil

Luke A. Parry[1,2*], Paulo C. Boggiani[3], Daniel J. Condon[4], Russell J. Garwood[5,6], Juliana de M. Leme[3], Duncan McIlroy[7], Martin D. Brasier[8], Ricardo Trindade[9], Ginaldo A. C. Campanha[3], Mírian L. A. F. Pacheco[10], Cleber Q. C. Diniz[3] and Alexander G. Liu[11]

The evolutionary events during the Ediacaran–Cambrian transition (~541 Myr ago) are unparalleled in Earth history. The fossil record suggests that most extant animal phyla appeared in a geologically brief interval, with the oldest unequivocal bilaterian body fossils found in the Early Cambrian. Molecular clocks and biomarkers provide independent estimates for the timing of animal origins, and both suggest a cryptic Neoproterozoic history for Metazoa that extends considerably beyond the Cambrian fossil record. We report an assemblage of ichnofossils from Ediacaran–Cambrian siltstones in Brazil, alongside U–Pb radioisotopic dates that constrain the age of the oldest specimens to 555–542 Myr. X-ray microtomography reveals three-dimensionally preserved traces ranging from 50 to 600 μm in diameter, indicative of small-bodied, meiofaunal tracemakers. Burrow morphologies suggest they were created by a nematoid-like organism that used undulating locomotion to move through the sediment. This assemblage demonstrates animal–sediment interactions in the latest Ediacaran period, and provides the oldest known fossil evidence for meiofaunal bilaterians. Our discovery highlights meiofaunal ichnofossils as a hitherto unexplored window for tracking animal evolution in deep time, and reveals that both meiofaunal and macrofaunal bilaterians began to explore infaunal niches during the late Ediacaran.

The Lower Cambrian fossil record documents a major radiation of macroscopic animals (particularly bilaterian phyla), coupled with significant expansion of their behavioural interactions with substrates and other organisms[1,2]. However, a growing catalogue of evidence from body fossils, trace fossils, biomarkers and molecular clocks indicates a protracted Neoproterozoic history for the Metazoa, with the origin of animals significantly pre-dating the base of the Cambrian[3].

A range of biological phenomena typically associated with animals first appears during the late Ediacaran interval (~580–541 Myr ago (Ma)), including skeletogenesis[4], reef building[5] and macroscopic predation[6]. Body fossils of late Ediacaran macro-organisms include at least some early animals[3], but crucially, most plausible claims for metazoans lie within the diploblasts rather than the Bilateria[3]. *Kimberella*, which is potentially a stem mollusc[7], is a notable exception, but some authors suggest that it can only be reliably considered as a member of total group Bilateria[3].

Our understanding of early animal evolution is complemented by ichnological investigations of latest Ediacaran to Ordovician strata[1,2,8]. Diverse ichnofossil assemblages in the earliest Cambrian place an important constraint on the tempo of bilaterian origins, as they indicate that some groups, including total group panarthropods and priapulid-like scalidophorans[2,9], were globally distributed and abundant by this point. The major bilaterian divergences (that is, the protostome–deuterostome and ecdysozoan–lophotrochozoan divergences) must therefore pre-date the Ediacaran–Cambrian boundary. So far, the Ediacaran trace fossil record has provided limited insight into these early divergences. Most Ediacaran ichnofossils are either surface traces or simple under-mat burrows, created either on or immediately beneath matgrounds[10]. Such traces extend back to ~565 Ma[11,16], including inferred grazing traces (*Kimberichnus*[12]) associated with the body fossil *Kimberella*, vertical adjustment structures in response to seafloor aggradation[13] and, in the latest Ediacaran, shallow vertical burrows[10] and treptichnid-like burrows just below the Ediacaran–Cambrian boundary[14]. Most Ediacaran ichnofossils are considered to have been made by total group bilaterian[15] or cnidarian[13,16] eumetazoans. Notwithstanding controversial claims for bioturbation and complex burrows ~553 Ma[17], widespread substrate-penetrating burrows capable of significant sediment mixing do not appear until close to the Precambrian–Cambrian boundary[14].

Molecular clock analyses predict an earlier, pre-Ediacaran origin for the Metazoa and Eumetazoa, and an early Ediacaran origin for Bilateria, Protostomia and Deuterostomia[18]. Palaeontological

[1]Palaeobiology, Royal Ontario Museum, 100 Queen's Park, Toronto, Ontario M5S 2C6, Canada. [2]Department of Ecology and Evolutionary Biology, University of Toronto, 25 Willcocks Street, Toronto, Ontario M5S 3B2, Canada. [3]Instituto de Geociências, Universidade de São Paulo, Rua do Lago, 562, 05508-080 São Paulo, Brazil. [4]NERC Isotope Geosciences Laboratory, British Geological Survey, Keyworth, Nottinghamshire NG12 5GG, UK. [5]School of Earth and Environmental Sciences, University of Manchester, Manchester M13 9PL, UK. [6]Department of Earth Sciences, Natural History Museum, Cromwell Road, London SW7 5BD, UK. [7]Department of Earth Sciences, Memorial University of Newfoundland, Alexander Murray Building, 300 Prince Philip Drive, St. John's, Newfoundland and Labrador A1B 3X5, Canada. [8]Department of Earth Sciences, University of Oxford, South Parks Road, Oxford OX1 3AN, UK. [9]Departamento de Geofisica, Instituto de Astronomia, Geofísica e Ciências Atmosféricas, Universidade de São Paulo, Rua do Matão 1226, 05508-900 São Paulo, Brazil. [10]Department of Biology, Federal University of São Carlos. Rodovia João Leme dos Santos - Parque Reserva Fazenda Imperial, Km 104, 18052780 Sorocaba, Brazil. [11]Department of Earth Sciences, University of Cambridge, Downing Street, Cambridge CB2 3EQ, UK. Martin D. Brasier is deceased. *e-mail: lparry@rom.on.ca

support for these suggestions is limited to purported body fossils of sponges[19] and demosponge biomarkers[20]. A considerable gap therefore remains between the fossil record of the late Ediacaran and molecular clock estimates for deep splits in the animal tree, for example the origin of Metazoa and Eumetazoa[3]. Assuming that contemporary molecular clock analyses yield accurate, if imprecise[18], node ages for animal divergences, a small body size and concomitant limited fossilization potential[21] could reconcile these discordant records of animal evolution (but see ref. [22]).

The small body size of the ancestral bilaterian is supported by recent phylogenomic analyses of deep animal relationships, with acoel flatworms and xenoturbellids (Xenacoelomorpha) being a sister group to all remaining bilaterians (Nephrozoa)[23], and small-bodied spiralian taxa (the 'Platyzoa') recognized as a paraphyletic grade with respect to macroscopic trochozoans[24]. This suggests that early bilaterians and spiralians were small bodied, possibly meiofaunal, and moved using ciliary gliding.

Meiofauna comprises all organisms between 32 and 1,000 µm in size that inhabit pore-water-rich sediments in freshwater to deep-marine environments[25]. Modern meiofaunal communities include animals, foraminifera and some ciliates, and contribute significantly to sediment bioturbation and bioirrigation[26,27]. The meiofauna can be divided into permanent members (that is, animals with organisms of a small size adapted and restricted to the meiofaunal, interstitial realm) and temporary meiofauna (for example, the larvae of macrobiota)[25].

Despite its ecological and evolutionary importance, the deep-time record of the meiofauna has received little discussion, principally due to the low preservation potential of both meiofaunal body fossils and traces. Although meiofaunal burrows (sometimes described as burrow mottling or cryptobioturbation) have occasionally been reported from Cambrian to Recent sediments[26], they are rarely subjected to detailed study. Body fossil discoveries also reveal organisms inhabiting meiofaunal niches within Early Cambrian communities, highlighting the potential for their preservation within particular taphonomic windows[28,29].

Here we report a new assemblage of meiofaunal ichnofossils from siltstones of the Ediacaran–Cambrian Tamengo and Guaicurus formations, Corumbá Group, central western Brazil (Fig. 1). The age of the assemblage is constrained by U–Pb (zircon) isotope dilution thermal ionization mass spectrometry (ID-TIMS) dating of inter-stratified ash beds. The dates indicate that the Tamengo Formation specimens are late Ediacaran in age, and those in the Guaicurus Formation lie close to the Ediacaran–Cambrian boundary. Our results constitute the oldest documented meiofaunal burrows in the geological record, placing a constraint on the minimum age of this key ecological innovation.

The Corumbá Group

The Corumbá Group, part of the Southern Paraguay Belt, is a ~600-m-thick sedimentary unit comprising carbonate and siliciclastic facies deposited on a stable continental margin following a late Neoproterozoic rift event[30,31] (Fig. 1). The lowermost units of the Corumbá Group are the terrigenous Cadieus and Cerradinho formations, which are probably contemporaneous with the Puga Formation of the Amazon Craton[30] (and thus possibly Marinoan-equivalent). Stromatolitic dolostones and phosphorites of the Bocaina Formation lie above those siliciclastic units. The lower Corumbá Group is unconformably overlain by the fossiliferous dark organic-rich marls and limestones of the Tamengo Formation, and laminated siltstones of the Guaicurus Formation[31] (Fig. 1). A breccia horizon marks the base of the Tamengo Formation in several sections, and is concordantly overlain by interbedded mudstones and grainstones deposited in a shallow platform setting. The laminated calcareous siltstones of the Guaicurus Formation indicate deposition in a setting with low hydrodynamic energy, probably below fair-weather wave base. The sedimentary succession has previously yielded macroscopic body fossils including the scyphozoan-like *Corumbella werneri* and *Paraconularia*[4], along with *Cloudina lucianoi*, in the upper Tamengo Formation, and possible vendotaenid algae (*Eoholynia*) in the lowermost Guaicurus Formation[31] (Fig. 1).

Results

U–Pb geochronology. Three volcanic tuff horizons were sampled within the Corumbá Group (Fig. 1) and zircons from these tuffs were dated using U–Pb chemical abrasion ID-TIMS (CA-ID-TIMS) methods (see Methods for full methodology). An ash bed from the top of the Bocaina Formation (from Porto Morrinhos; Fig. 1) yielded a weighted mean $^{206}Pb/^{238}U$ date of 555.18 ± 0.30/0.34/0.70 Ma (mean square weighted deviation (MSWD) = 1.6, n = 8 out of 8) (Supplementary Fig. 6; Supplementary Tables 3 and 4), which we consider to approximate the age of the sample. This date provides a maximum age for the overlying Tamengo Formation. Two further ash beds (samples 1.08 and 1.04) were collected from the top of the Tamengo Formation. Zircons from sample 1.04 yielded U–Pb CA-ID-TIMS dates that ranged from 541.2 to 548 Ma, with a cluster of the five youngest concordant analyses defining a weighted mean $^{206}Pb/^{238}U$ date of 541.85 ± 0.75/0.77/0.97 Ma (MSWD = 3.3, n = 5 out of 11) (Supplementary Fig. 6; Supplementary Tables 3 and 4) that we consider approximates the age of the sample. Zircons from sample 1.08 yielded U–Pb CA-ID-TIMS dates that ranged from 537 to 552 Ma, with a coherent cluster of four concordant analyses (Fig. 2) defining a weighted mean $^{206}Pb/^{238}U$ date of 542.37 ± 0.28/0.32/0.68 Ma (MSWD = 0.68, n = 4 out of 8) (Supplementary Fig. 6; Supplementary Tables 3 and 4). We consider the single significantly older data point to result from the incorporation of xenocrystic zircon, perhaps during eruption. The three younger $^{206}Pb/^{238}U$ dates from sample 1.08 are considered to reflect Pb loss based on the observations that (1) they are non-overlapping; (2) the $^{207}Pb/^{206}Pb$ dates are similar to those that define the ~542 Ma population in both this sample and sample 1.04; and (3) the derived dates from both upper Tamengo Formation samples are consistent. Therefore 542.37 ± 0.28/0.32/0.68 Ma is taken to approximate the age of sample 1.08. The data from samples 1.04 and 1.08 indicate an age of ~542 Ma for the top of the Tamengo Formation, constraining the age of the upper Corumbá Group as late Ediacaran (uppermost Bocaina–Tamengo formations, 555–542 Ma) to earliest Cambrian (lower Guaicurus Formation, <542 Ma). The current accepted age for the base of the Cambrian is 541.00 ± 0.29 Ma[32] (level Y uncertainty, excluding the systematic ^{238}U decay constant uncertainty).

Trace fossils of the Guaicurus and Tamengo formations. Three-dimensionally mineralized fossils were collected from approximately 30–40 m above the base of the Tamengo Formation at two levels in the Ladário section (Fig. 1), and from a single horizon and loose material ~7 m above the base of the Guaicurus Formation from the Laginha Mine section (Fig. 1). The latter horizon is <542.0 Ma in age based on the U–Pb CA-ID-TIMS data presented above.

Bi-lobed horizontal, iron-oxide-filled ichnofossils occur in a single hand specimen, preserving part and counterpart, derived from float in the lower Guaicurus Formation (Fig. 2c,d). The burrows are straight to curving, approximately 2 mm in width, and exhibit dorsal and ventral median depressions, creating the bi-lobed appearance typical of *Didymaulichnus lyelli*[33].

Small sub-horizontal structures occur in abundance in both the lower Guaicurus (Fig. 2) and Tamengo formations (Fig. 3). These consist of irregular multi-tiered networks connected by short sub-vertical shafts. In bedding plane view, the fossils are dark in colour relative to the matrix, forming dense assemblages comprising sinuous structures with rare dichotomous branches (Fig. 2a,b). The fossils are filled with oxidized iron-rich minerals with framboidal morphologies, and authigenic microcrystalline calcite (Fig. 2e–h). Framboids suggest that the fossils were originally pyritized, and subsequently oxidized to iron oxides and oxyhydroxides

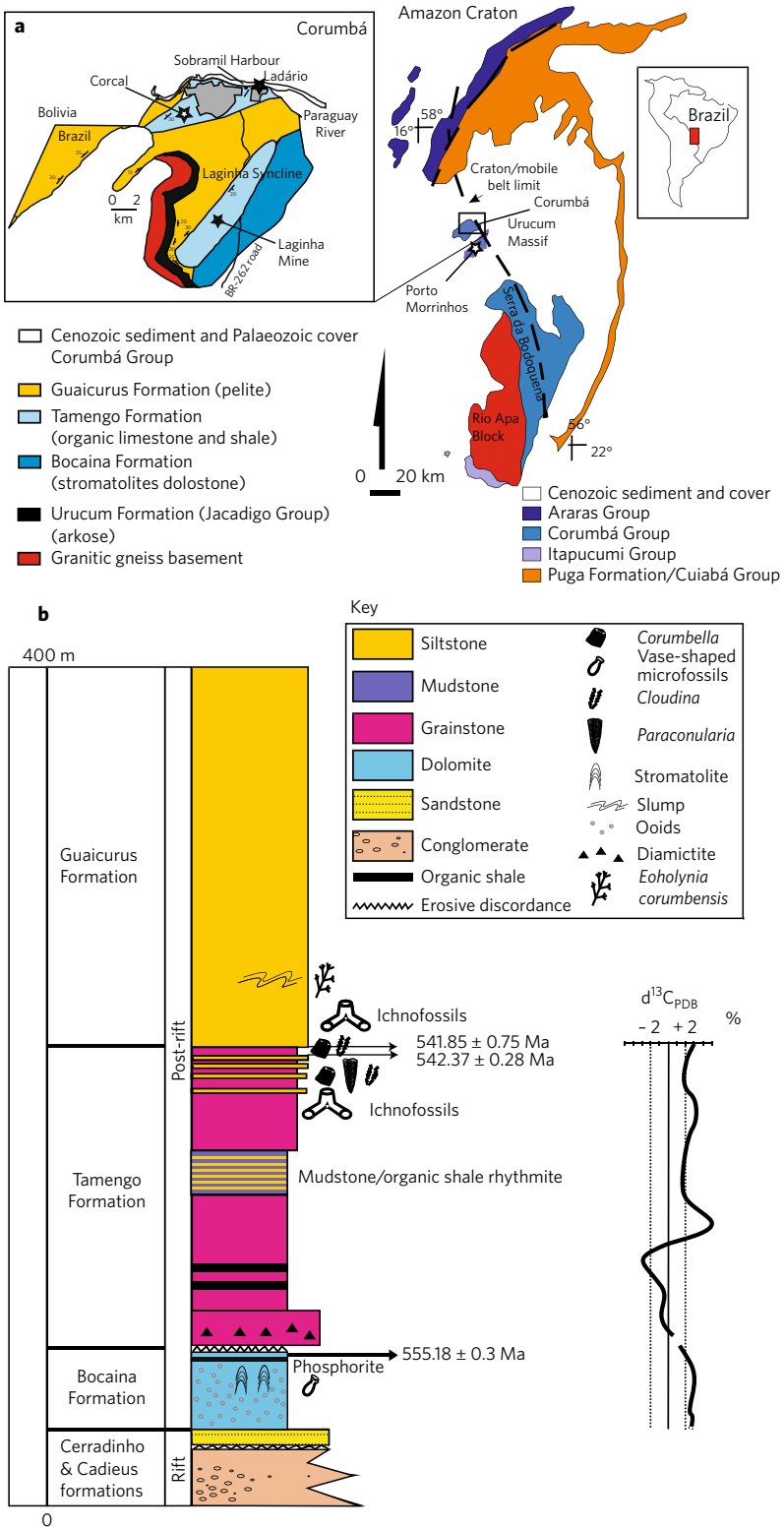

Fig. 1 | Locality map and stratigraphic column of the Ediacaran–Early Cambrian Corumbá Group: composite section compiled from logs in the Corumbá–Ladário region, Mato Grosso do Sul State, Brazil. a,**b**, Locality map (**a**) and stratigraphic column (**b**). Dates are derived from this study. White stars indicate localities from which samples for geochronology were obtained. Black stars indicate ichnofossil localities described in this study: Laginha Mine (Guaicurus Formation) 19° 07′ 09.8′′ S, 057° 38′ 40.4′′ W; Ladário (Tamengo Formation) 19° 0′ 04.0′′ S, 57° 36′ 00.7′′ W. Carbon isotope stratigraphy comes from the Laginha Mine section[52]. Age uncertainties are expressed as MSWD.

(Supplementary Fig. 1). The presence of calcite and framboids throughout the infill suggests that the framboids and calcite formed at a similar time.

The density contrast between the fossils and the host rock allows the traces to be visualized through X-ray microtomography (μCT; Figs. 3–5), revealing a dense ichnofabric (Figs. 3e–g, 4e,f and 5f).

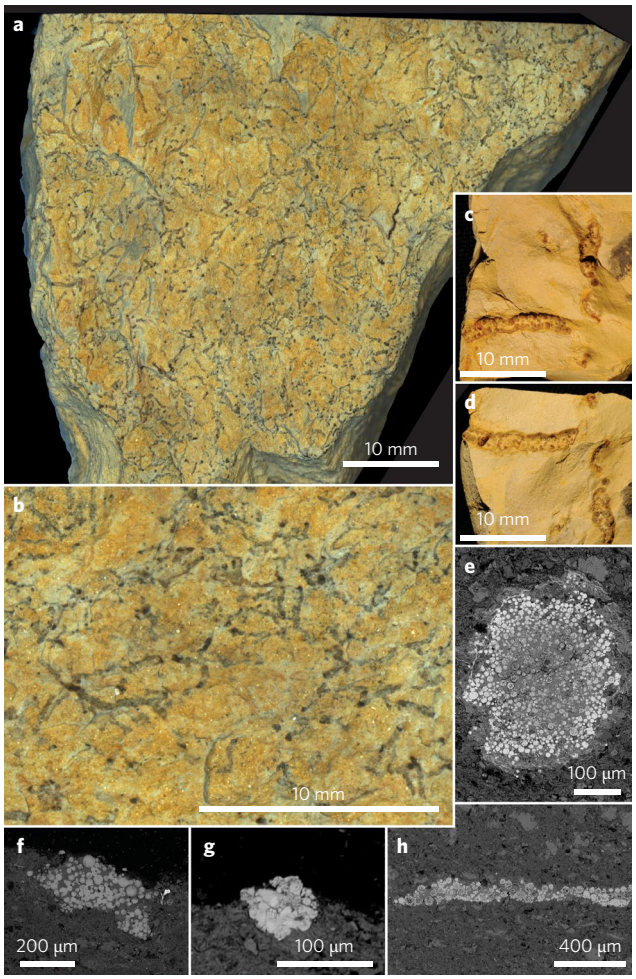

Fig. 2 | Hand specimens and scanning electron microscopy photomicrographs of *M. minima* and *D. lyelli* traces from the Guaicurus Formation, Laginha Mine, Mato Grosso do Sul State, Brazil. a, Hand specimen of small *M. minima*, OUMNH ÁU.4c. **b**, Bedding plane view of *M. minima* (inset of **a**). **c**,**d**, Bedding plane view of bi-lobed *D. lyelli* (part and counterpart, OUMNH ÁU.2). **e**–**h**, Scanning electron microscopy photomicrographs of bedding-normal polished thin sections of samples containing *M. minima*. Framboidal iron oxide (originally pyrite) burrow fills are clearly observed. Burrows in **e**–**g** are viewed in cross-section through the burrow diameter. **h**, A burrow in lateral view.

Although many of the burrows are restricted to single horizons, some cut across up to ~7 mm of stratigraphic thickness, indicating interstratal burrowing (Fig. 4g). Burrow diameters range from 45 to 573 µm (Fig. 5g; mean = 193.2 µm, $n = 393$). The Shapiro–Wilks test indicates these data are not drawn from a normal distribution ($P < 0.01$), and univariate Bayesian information criterion (BIC) analysis supports either a two- or three-component model. The lower limits of this distribution are probably dictated by the voxel size of the scans and so it is possible that the smallest size fractions are omitted.

Discussion

The Guaicurus Formation assemblage is dated at $< 541.85 \pm 0.77$ Ma and is broadly contemporaneous with the Ediacaran–Cambrian boundary[32]. The Tamengo Formation ichnofossils lie stratigraphically below our dated horizon of 542.37 ± 0.32 Ma, and are thus between 542 and 555 Ma in age (late Ediacaran). The presence of different size classes within the Corumbá Group data indicates different populations, further supporting a biological, rather than abiological, mode of formation (see Supplementary Information). As the structures are preserved as discrete, rounded authigenically mineralized tubes, they cannot be shrinkage features such as synaeresis cracks.

A body fossil explanation for these structures is considered unlikely as authigenically mineralized body fossils (for example, algal filaments) would be expected to be confined to discrete horizons in finely laminated sediments rather than crossing multiple horizons. Some Ediacaran body fossils, such as the simple conical *Conotubus*, can grow through sedimentary laminae if felled[34]. In contrast, the branching ichnofossils of the Guaicurus Formation are ~0.5 mm wide and cross up to ~7 mm of stratigraphic thickness. The contemporaneous (Fig. 1) vendotaenid alga *Eoholynia corumbensis* is superficially similar in size and morphology to the ichnofossils described herein[31]. Two factors make algal origins for the fossils we describe unlikely: mode of preservation, and morphology. First, in contrast to these authigenically mineralized trace fossils, *Eoholynia* specimens in the Corumbá Group are preserved as two-dimensional (2D) carbon films with some accessory oxides (possibly after pyrite) (Supplementary Fig. 5d–f). A comprehensive study of early Palaeozoic non-biomineralized macroalgal taxa found that 2D compression (with some accessory mineralization) is the only taphonomic pathway through which macroalgae fossilize during this time interval[35], consistent with the algal affinities of *Eoholynia* and similar fossils. Although taphonomic mode should not be conflated with affinity, the absence of three-dimensionally pyritized algae from similar localities of the same age renders an algal affinity for the proposed ichnofossils unlikely. Secondly, *Eoholynia* have straight branches (rather than undulating/sinusoidal) that taper after regular (dichotomous to polychotomous) branching from a distinct main branch and have rounded terminal structures interpreted as sporangia[31]. Polychotomous branching, tapering and rounded termini are not present in the ichnofossils.

Iron oxides form a patina on the outer margin of some larger endichnial burrows, possibly reflecting pyritization of a mucous burrow lining[36] (Fig. 2e). 3D preservation as authigenic pyrite and calcite suggests that the burrows were open prior to burial and compaction, and were not backfilled by the tracemaker. Preservation in almost undistorted full relief is uncommon in mudstones in the absence of burrow fill, except where significant early diagenesis and dewatering occurs before burial[36]. Similar sized burrows of modern nematodes possess a polysaccharide-rich mucous burrow lining[37], which would provide a locus for the microbial reduction of sulfate from seawater within the burrows, causing pyrite precipitation and consequently burrow preservation[38]: a mechanism we consider to have been responsible for preservation of the Corumbá Group structures.

The poorly organized, vertically stacked, network-like galleries connected by short oblique shafts are typical of the ichnogenus *Multina*. A combination of size range and irregularly sinuous gallery morphology allows attribution to *M. minima*[39]. The small burrow diameter, originally circular cross-sections and lack of dorso-ventral differentiation characteristic of the Corumbá Group *Multina* are consistent with a narrow-bodied vermiform tracemaker. It is unclear how many infaunalization events are represented by the assemblages reconstructed in 3D (for example, Fig. 5e), but the presence of continuous oblique shafts between levels suggests that the burrows remained open throughout the life of the tracemaker.

Animal burrowing is typically achieved either (1) by peristalsis (for example, in annelids like the Arenicolidae); (2) through the extension and retraction of an introvert (for example, loriciferans, kinorynchs, sipunculans); or (3) by a combination of the two (for example, priapulids)[40]. These mechanisms compact sediment laterally at the burrow margins[41], but such compaction is absent in the Guaicurus traces (Fig. 2e–g). Compression burrowing is similar and involves the tracemaker forcing its way through the sediment, compacting it at the margins[42]. Trochozoan taxa

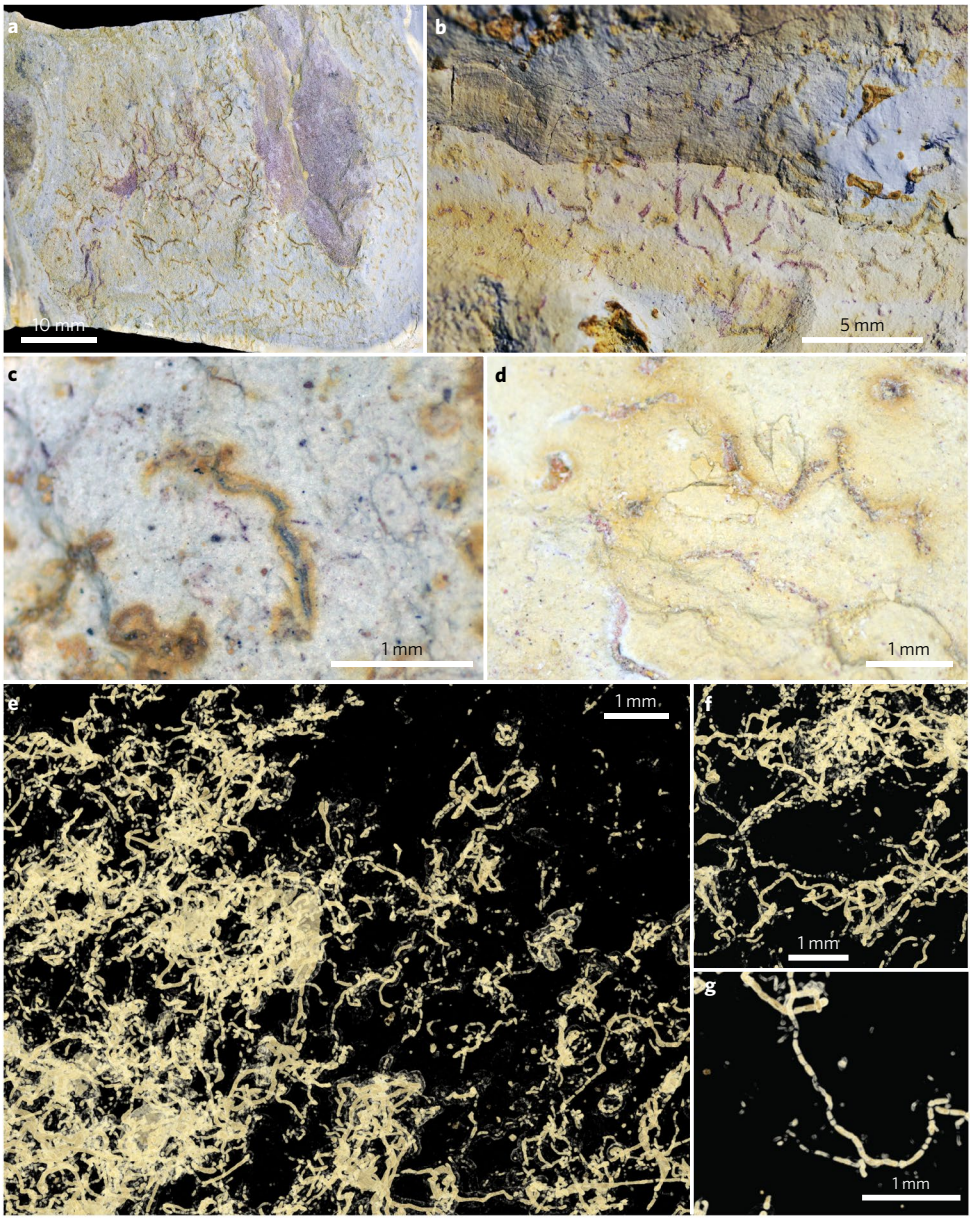

Fig. 3 | Photographs and CT volume renders of *M. minima* burrows from the Ediacaran Tamengo Formation, Ladário, Mato Grosso do Sul State, Brazil. **a**, Representative hand specimen of Tamengo Formation samples, specimen GPIE 11048b. **b**–**d**, Oxidized burrows with sub-horizontal trajectories, viewed in plan view on a bedding surface, GPIE-11048b (**b**), GPIE-11004b (**c**) and GPIE-11005a (**d**). Note that these specimens have been heavily weathered. **e**–**g**, Volume renders of CT slice data through the burrows constructed using the program Drishti. The burrows show curved, sub-horizontal trajectories, and are mostly <100 µm in diameter.

such as annelids, molluscs and nemerteans can be excluded as potential tracemakers because the minimum diameter *M. minima* resolved in the Guaicurus Formation is ~45 µm; significantly smaller than recently hatched trochophore larvae, which are approximately 100 µm in diameter and pelagic, not endobenthic[43]. Annelids can be further excluded as potential tracemakers as the smallest annelid eggs (50–70 µm diameter[43]) exceed the diameter of the smallest traces.

Early spiralians may have been small bodied, with taxa such as gastrotrichs and gnathiferans recovered as a paraphyletic grade in phylogenomic analyses[24]. Many spiralian meiofaunal groups move using ciliary gliding, which is unlikely to have formed continuous open burrows or achieved the sediment movement responsible for interstratal burrowing. Mucociliary gliding by extant platyhelminths[44] creates traces similar in gross morphology to horizontal Ediacaran trails, and so members of the total groups of Bilateria, Xenacoelomorpha and Nephrozoa are candidate tracemakers for late Ediacaran surficial traces. Ciliary gliding has probably been independently lost multiple times within Nephrozoa (for example, Ecdysozoa, which lack external ciliation). Ciliary gliding is retained in some macroscopic spiralians, including Nemertea, Platyhelminthes and molluscan classes in which the foot is used in locomotion, such as gastropods. Nevertheless, ciliary gliding was the probable locomotory mechanism for the last common ancestor of both Bilateria and Nephrozoa. Ciliary gliding is unlikely to produce open burrows in fine-grained sediments and in the meiofauna it is most commonly used by organisms that live in interstitial spaces between sand grains.

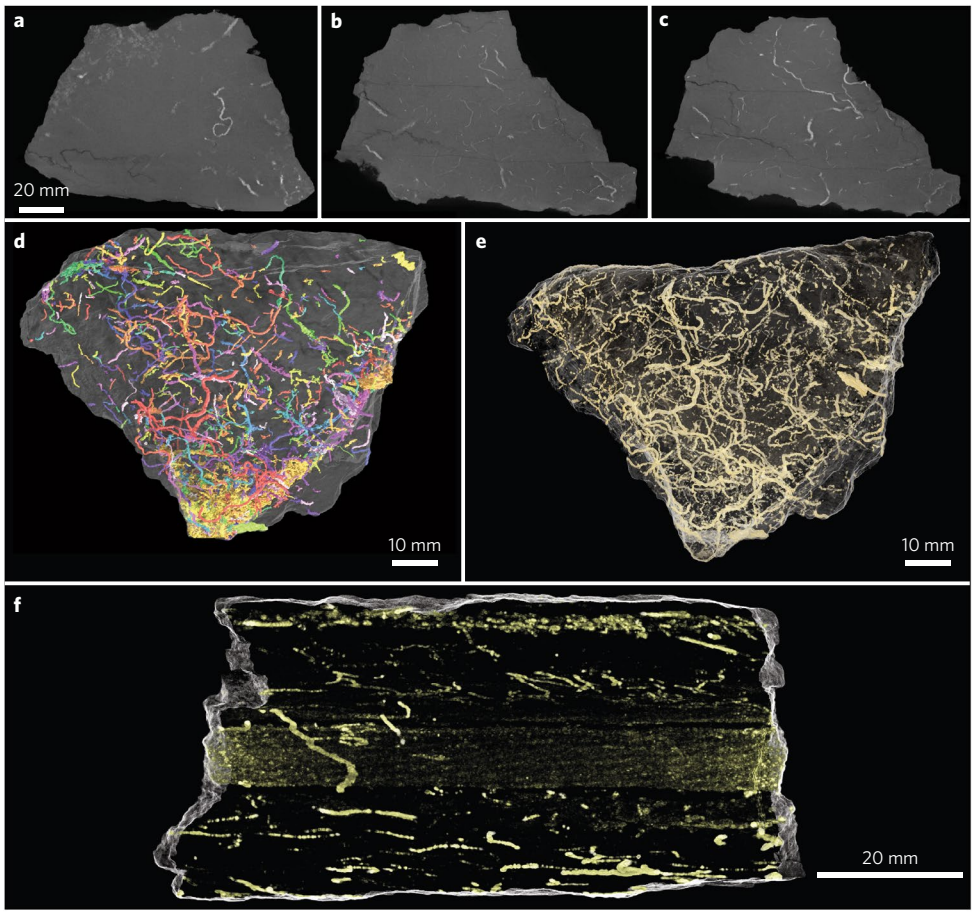

Fig. 4 | CT slices and 3D reconstructions of a burrow assemblage in specimen OUMNH ÁU.3 from the Early Cambrian/latest Ediacaran Guaicurus Formation. a–c, Representative CT X-ray slices through the specimen in plan view, showing burrows in light grey against a dark grey rock matrix. Scale bar in **a** also applies to **b** and **c**. **d**, 3D render of the specimen produced using Blender, showing individual burrows in different colours. **e**, The same CT data volume rendered in Drishti, with burrows in gold. **f**, Drishti volume render normal to bedding, showing interstratal burrowing.

Free-living nematodes use undulating motions to move through fine-grained soft sediments, the low viscosity of which limits them to small body size[45]. Organisms without body appendages possessing only longitudinal muscles, such as nematodes[46], are restricted to sinusoidal locomotion as they lack the antagonistic circular muscles necessary for peristalsis. Nematodes are common bioturbators of modern muddy sediments and can create open mucus-lined burrows of a size range comparable to that of the Brazilian *M. minima* (Fig. 5g). Similar but slightly larger *M. minima*, potentially attributable to marine nematodes, have been described from the Cambrian and Ordovician[47,48], but do not preserve the tiered networks of *M. minima* we report. Burrow morphologies produced by extant or extinct nematomorphs are unknown.

The size and morphology of the meiobenthic *Multina* is consistent with a nematoid-like tracemaker that lacked body appendages and did not move by peristalsis or ciliary gliding. As the ancestral bilaterian and nephrozoan moved using ciliary gliding, this burrowing style suggests a tracemaker that phylogenetically postdates the nephrozoan crown node. These burrows may potentially provide an age constraint for total group Nematoida (that is, nematodes plus nematomorphs). This is consistent with Early Cambrian body fossils, which include representatives of most ecdysozoan phyla, along with meiofaunal groups[28]. Total group nematoids are therefore likely to have diverged from their closest living relatives by at least 520 Ma, regardless of their controversial position within Ecdysozoa[49]. An alternative interpretation is that these trace fossils were produced by a stem group ecdysozoan that phylogenetically pre-dates the evolution of an introvert but had already evolved a chitinous cuticle and thus was unable to use ciliary gliding. A similar body plan is present in larval insects, which produce freshwater and terrestrial *Cochlichnus* burrows and move in a similar fashion to nematodes[10].

The Proterozoic–Phanerozoic biological radiation and the origin of the meiofauna. The Corumbá Group trace fossils place an important latest Ediacaran (541–555 Ma) minimum constraint on the origin of meiofaunal animals and their interactions with soft substrates. Meiofauna are ubiquitous in both modern marine and freshwater environments, and their origin in deep time has been often discussed[21,22] but little explored from an evidential palaeontological perspective. Extant meioendobenthic organisms are particularly important contributors to biogeochemical cycling, microbial ecology and ecosystem productivity, especially in muddy sediments[27,37]. Multiple studies discuss the trace fossil record of macrofaunal behaviour from the late Ediacaran onwards, its postulated impacts on sediment geochemistry and benthic ecology, and its role in ecosystem engineering and ecological escalation[1,2,8]. Constraining the deep time origins of a meiofaunal mode of life may be equally important for understanding the biological and chemical evolution of marine sedimentary environments. It is unlikely that the meiofaunal burrowing described here had a substantial impact on substrate mixing, due to its small depth of penetration leaving sedimentary laminae largely undisturbed (Fig. 4e).

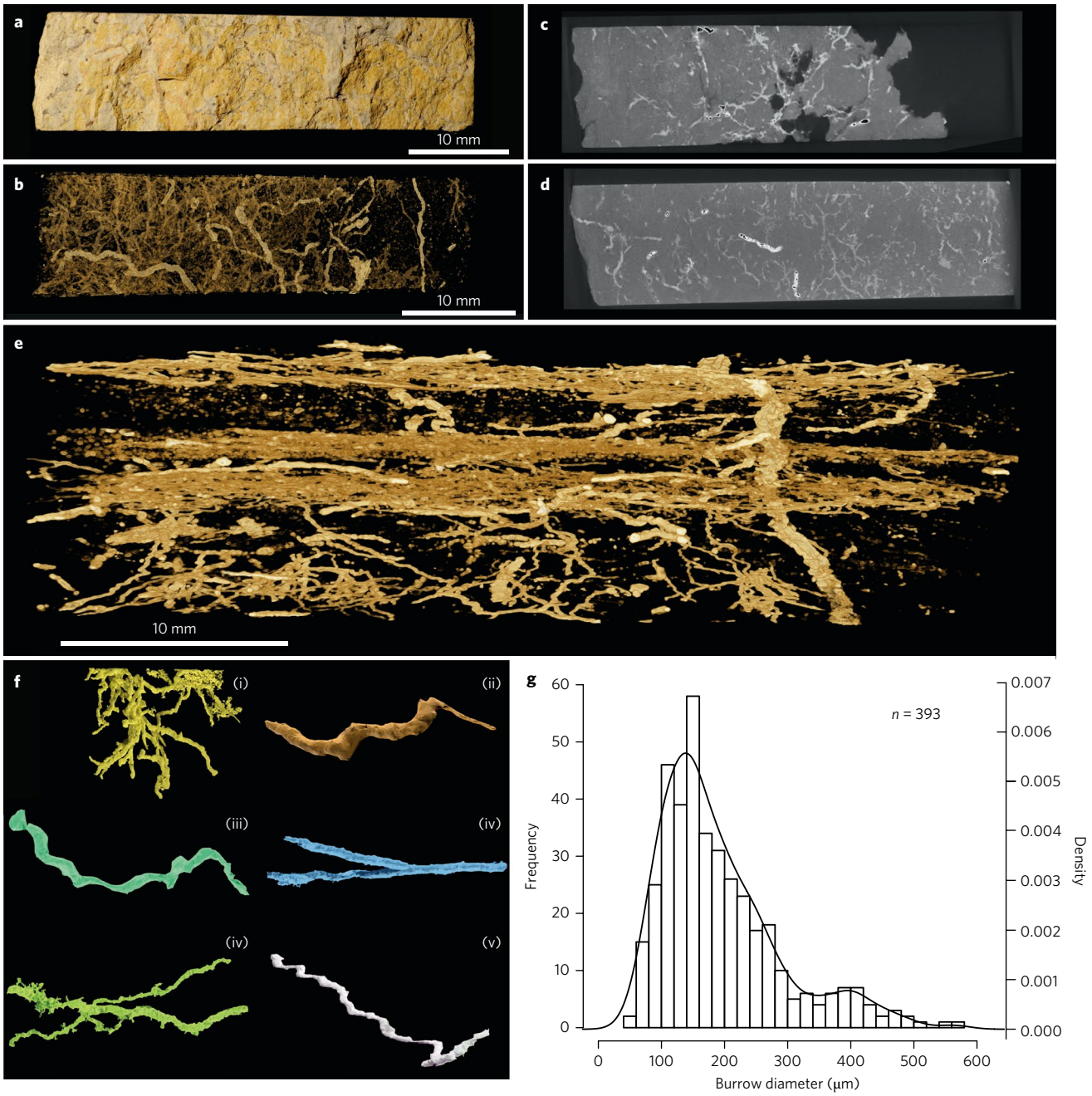

Fig. 5 | Specimen OUMNH ÁU.4/p1 from the Guaicurus Formation from which burrow measurement data were obtained. a, Hand specimen from the Laginha Mine section, plan view. **b**, Drishti volume render of 3D CT scan data, plan view. **c**,**d**, Individual CT slices in plan view, from which burrow measurements were obtained via comparison of 3D volume render to determine the maximum diameter of each burrow. Scale bar as in **b**. **e**, The Drishti volume render in **b** in lateral view. **f**, Individual burrow morphologies extracted from the volume render in **b**. **g**, Histogram plotting burrow width against frequency.

Our geochronological framework places temporal constraints on the first appearance of several biological and ecological innovations in the South American fossil record, and permits correlation of these events to other dated sections worldwide (Fig. 6). Biomineralizing macro-organisms (*Cloudina*), annulated tubular macrofossils (*Corumbella*) and meiofaunal burrowers all appear in the Corumbá sections after 555 Ma, but before 542 Ma. The temporal range for the macrofossils corresponds well to similar latest Ediacaran fossil assemblages, some of which record evidence for predation[50], a decline in Ediacaran soft-bodied macro-organisms[51] and the appearance of macroscopic burrows[10,17] in the interval immediately preceding the Ediacaran–Cambrian boundary. Taken together, these records bear witness to several major biological innovations among eumetazoans, indicating that this key interval may offer significant scope for unravelling the intricacies surrounding the early stages of bilaterian evolution.

Methods

U–Pb geochronology. U–Pb dates were obtained by the CA-ID-TIMS method on selected single zircon grains (Supplementary Tables 3 and 4), extracted from an aliquot of samples 'Porto Morrinhos', '1.04' and '1.08'. Zircon grains were

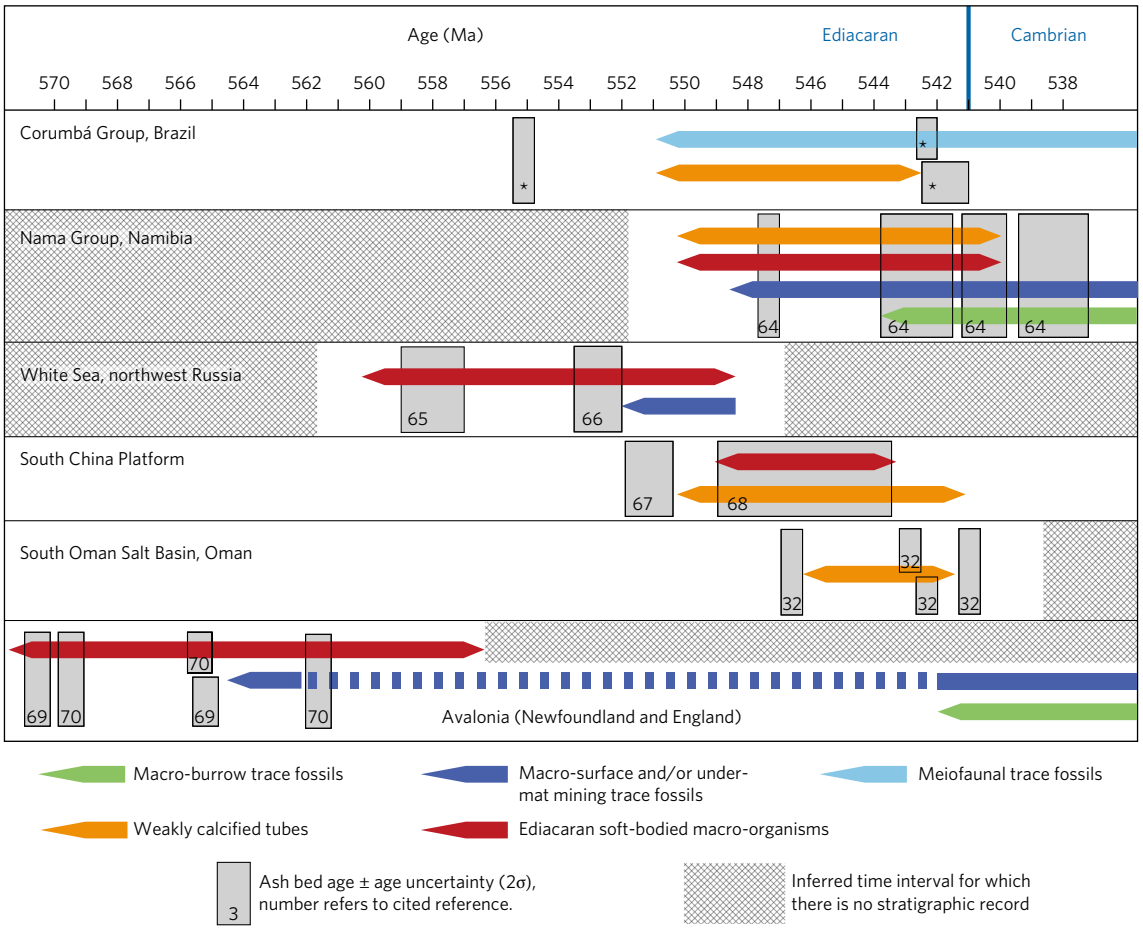

Fig. 6 | Plot showing the temporal distribution of body and trace fossils from key Ediacaran and earliest Cambrian stratigraphic sections that are radio-isotopically constrained to a useful level of precision. Uncertainty in the temporal occurrence of a given fossil is constrained by dated ash layers that occur above or below the fossil type occurrence. The uncertainty in the placement of the first and last occurrence datum increases away from the dated levels. *Data from this study.

isolated from the rock samples using standard magnetic and density separation techniques, and annealed in a muffle furnace at 900 °C for 60 h in quartz beakers. Zircon crystals from sample Porto Morrinhos have aspect ratios varying from ~2 to ~5 and are typically 150 to 300 µm in their longest dimension, and often contained a medial melt inclusion typical of volcanic zircon. Zircon from samples 1.04 were smaller, with the long dimension of the order of 50 to 100 µm, with lower aspect ratios (~2) and were doubly terminated. Zircon from samples 1.08 had aspect ratios ranging from 2 to 4, long dimension of the order of 100 to 200 µm and were doubly terminated. No cathodoluminescence imaging was undertaken due to the small size of the zircons, and because the presence of medial melt inclusions and the general external morphologies were indicative of inherited cores not being present. Zircons selected for analyses based on external morphology were transferred to 3 ml Teflon PFA beakers, washed in dilute HNO_3 and water, and loaded into 300 µl Teflon PFA microcapsules. Fifteen microcapsules were placed in a large-capacity Parr vessel, and the crystals partially dissolved in 120 µl of 29 M HF for 12 h at 180 °C. The contents of each microcapsule were returned to 3 ml Teflon PFA beakers, the HF removed and the residual grains immersed in 3.5 M HNO_3, ultrasonically cleaned for an hour, and fluxed on a hotplate at 80 °C for an hour. The HNO_3 was removed and the grains were rinsed twice in ultrapure H_2O before being reloaded into the same 300 µl Teflon PFA microcapsules (rinsed and fluxed in 6 M HCl during crystal sonication and washing) and spiked with the EARTHTIME mixed ^{233}U–^{235}U–^{205}Pb tracer solution (ET535). These chemically abraded grains were dissolved in Parr vessels in 120 µl of 29 M HF with a trace of 3.5 M HNO_3 at 220 °C for 60 h, dried to fluorides and then re-dissolved in 6 M HCl at 180 °C overnight. U and Pb were separated from the zircon matrix using an HCl-based anion exchange chromatographic procedure, eluted together and dried with 2 µl of 0.05 N H_3PO_4. Pb and U were loaded on a single outgassed Re filament in 5 µl of a silica gel/phosphoric acid mixture[53], and U and Pb isotopic measurements made on a Thermo Triton multi-collector thermal ionization mass spectrometer equipped with an ion-counting secondary electron multiplier (SEM) detector. Pb isotopes were measured by peak-jumping all isotopes on the SEM detector for 100 to 150 cycles. Pb mass fractionation was externally corrected using a mass bias factor of 0.14 ± 0.03% per mass unit determined via measurements of $^{202}Pb/^{205}Pb$ (ET2535)-spiked samples analysed during the same experimental period. Transitory isobaric interferences due to high-molecular-weight organics, particularly on ^{204}Pb, disappeared within approximately 30 cycles or earlier, and ionization efficiency averaged 10^4 cps pg^{-1} of each Pb isotope. Linearity (to $\geq 1.4 \times 10^6$ cps) and the associated deadtime correction of the SEM detector were monitored by repeated analyses of NBS982, and have been constant since installation in 2006. Uranium was analysed as UO_2^+ ions in static Faraday mode on 10^{12} Ω resistors for 150 to 200 cycles, and corrected for isobaric interference of $^{233}U^{18}O^{16}O$ on $^{235}U^{16}O^{16}O$ with an $^{18}O/^{16}O$ ratio of 0.00206. Ionization efficiency averaged 20 mV ng^{-1} of each U isotope. U mass fractionation was corrected using the known $^{233}U/^{235}U$ ratio of the ET2535 tracer solution.

We used the ET535 tracer solution[54,55] and U decay constants recommended in ref. [56]. A value of 137.818 ± 0.045 was used for the $^{238}U/^{235}U_{zircon}$ based on the work of ref. [57]. $^{206}Pb/^{238}U$ ratios and dates were corrected for initial ^{230}Th disequilibrium using a $Th/U_{magma} = 3 \pm 1$ resulting in an increase in the $^{206}Pb/^{238}U$ dates of ~0.09 Myr. All common Pb in analyses was attributed to laboratory blank and subtracted based on the measured laboratory Pb isotopic composition and associated uncertainty. U blanks were estimated at 0.1 pg, based on replicate total procedural blanks.

Here, the date uncertainties reporting is as X/Y/Z and reflects the following sources: (X) analytical, (Y) analytical + tracer solution and (Z) analytical + tracer solution + decay constants. The X uncertainty is the internal error based on only analytical uncertainties, including counting statistics, subtraction of tracer solution, and blank and initial common Pb subtraction. It is given at the 2σ confidence interval. This error should be considered when comparing our dates with $^{206}Pb/^{238}U$ dates from other laboratories that used the same EARTHTIME tracer solution or a tracer solution that was cross-calibrated using related gravimetric reference materials. The Y uncertainty includes uncertainty in the tracer calibration and

should be used when comparing our dates with those derived from laboratories that did not use the same EARTHTIME tracer solution or a tracer solution that was cross-calibrated using relatable gravimetric reference material. The Z uncertainty includes the above in addition to uncertainty in the ^{238}U decay constant[56]. This uncertainty level should be used when comparing our dates with those derived from other decay schemes (for example, $^{40}Ar/^{39}Ar$, $^{187}Re–^{187}Os$).

CT. Four individual hand specimens were scanned using Nikon XTH-225 µCT scanners at the Natural History Museum (London), and the Life Sciences Building, University of Bristol. X-rays were generated using a tungsten target. Scan parameters are provided in the Supplementary Information.

Following µCT scanning, the data were imported into the program Drishti. We used this program both to volume render the data following the methods in ref. [58] and to reslice the volumes to create a TIFF stack of images approximately parallel to bedding. The data were also segmented using the SPIERS software suite[59] following the methods of ref. [60], exported as stereolithography meshes, and then imported into the open source raytracer Blender[40]. In Blender, the mesh of the surface was rendered partially transparent, and the mesh encompassing all burrows was split into its component islands, allowing them to be coloured separately.

Burrow measurements. No statistical methods were used to predetermine sample size. Burrow measurements were obtained using ImageJ[61]. Measurements of burrow diameter were taken from individual slices from specimen OUMNH ÁU.3, to characterize the size frequency distribution of the trace fossils (Fig. 5g). Burrows were measured from approximately bedding-parallel µCT slices at maximum burrow width. This was preferred over systematically measuring burrows from a sample of slices, as such a method would not necessarily sample burrows at their maximum diameter, and consequently would skew the size frequency distribution towards a smaller mean diameter. The smallest burrows observed in µCT slices are approximately 2 pixels (~40 µm) in diameter, and are thus at the limit of scan resolution. A Shapiro–Wilks test and BIC analysis (using the R package mclust[62]) were used to determine population structure in the measurement data[63].

Data availability. U–Pb isotopic data used in this study are available in the Supplementary Information. CT data are freely available at Zenodo (doi: 10.5281/zenodo.842847). All specimens analysed are held at the University of Sao Paulo and Oxford University Museum of Natural History.

Received: 8 December 2016; Accepted: 28 July 2017;
Published online: 11 September 2017

References

1. McIlroy, D. & Logan, G. A. The impact of bioturbation on infaunal ecology and evolution during the Proterozoic–Cambrian transition. *Palaios* **14**, 58–72 (1999).
2. Mángano M. G. & Buatois, L. A. Decoupling of body-plan diversification and ecological structuring during the Ediacaran–Cambrian transition: evolutionary and geobiological feedbacks. *Proc. R. Soc. B* **281**, 20140038 (2014).
3. Cunningham, J. A., Liu, A. G., Bengtson, S. & Donoghue, P. C. The origin of animals: can molecular clocks and the fossil record be reconciled? *Bioessays* **39**, 1–12 (2017).
4. Van Iten, H. et al. in *The Cnidaria, Past, Present and Future* (eds Goffredo, S. & Dubinsky, Z.) 31–40 (Springer, Berlin, 2016).
5. Penny, A. M. et al. Early animals. Ediacaran metazoan reefs from the Nama Group, Namibia. *Science* **344**, 1504–1506 (2014).
6. Bengtson, S. & Zhao, Y. Predatorial borings in Late Precambrian mineralized exoskeletons. *Science* **257**, 367–369 (1992).
7. Vinther, J., Parry, L., Briggs, D. E. G. & Van Roy, P. Ancestral morphology of molluscs revealed by a new Ordovician stem aculiferan. *Nature* **542**, 471–474 (2017).
8. Tarhan, L. G., Droser, M. L., Planavsky, N. J. & Johnston, D. T. Protracted development of bioturbation through the early Palaeozoic era. *Nat. Geosci.* **8**, 865–869 (2015).
9. Vannier, J., Calandra, I., Gaillard, C. & Żylińska, A. Priapulid worms: pioneer horizontal burrowers at the Precambrian–Cambrian boundary. *Geology* **38**, 711–714 (2010).
10. Buatois, L. A. & Mángano, M. G. *Ichnology: Organism–Substrate Interactions in Space and Time* (Cambridge Univ. Press, Cambridge, 2011).
11. Jensen, S. The Proterozoic and earliest Cambrian trace fossil record; patterns, problems and perspectives. *Integr. Comp. Biol.* **43**, 219–228 (2003).
12. Gehling, J. G., Runnegar, B. N. & Droser, M. L. Scratch traces of large Ediacara bilaterian animals. *J. Paleontol.* **88**, 284–298 (2014).
13. Menon, L. R., McIlroy, D. & Brasier, M. D. Evidence for Cnidaria-like behavior in ca. 560 Ma Ediacaran *Aspidella*. *Geology* **41**, 895–898 (2013).
14. Jensen, S., Saylor, B. Z., Gehling, J. G. & Germs, G. J. Complex trace fossils from the terminal Proterozoic of Namibia. *Geology* **28**, 143–146 (2000).
15. Chen, Z. et al. Trace fossil evidence for Ediacaran bilaterian animals with complex behaviours. *Precambrian Res.* **224**, 690–701 (2013).
16. Liu, A. G., McIlroy, D. & Brasier, M. D. First evidence for locomotion in the Ediacara biota from the 565 Ma Mistaken Point Formation, Newfoundland. *Geology* **38**, 123–126 (2010).
17. Rogov, V. et al. The oldest evidence of bioturbation on Earth. *Geology* **40**, 395–398 (2012).
18. dos Reis, M. et al. Uncertainty in the timing of origin of animals and the limits of precision in molecular timescales. *Curr. Biol.* **25**, 2939–2950 (2015).
19. Yin, Z. et al. Sponge grade body fossil with cellular resolution dating 60 Myr before the Cambrian. *Proc. Natl Acad. Sci. USA* **112**, E1453–E1460 (2015).
20. Love, G. D. & Summons, R. E. The molecular record of Cryogenian sponges–a response to Antcliffe (2013). *Palaeontology* **58**, 1131–1136 (2015).
21. Fortey, R. A., Briggs, D. E. G. & Wills, M. A. The Cambrian evolutionary 'explosion' recalibrated. *BioEssays* **19**, 429–434 (1997).
22. Budd, G. E. & Jensen, S. A critical reappraisal of the fossil record of the bilaterian phyla. *Biol. Rev.* **75**, 253–295 (2000).
23. Cannon, J. T. et al. Xenacoelomorpha is the sister group to Nephrozoa. *Nature* **530**, 89–93 (2016).
24. Laumer, C. E. et al. Spiralian phylogeny informs the evolution of microscopic lineages. *Curr. Biol.* **25**, 2000–2006 (2015).
25. Giere, O. *Meiobenthology: The Microscopic Motile Fauna of Aquatic Sediments* (Springer Science & Business Media, Berlin, 2008).
26. Löhr, S. & Kennedy, M. Micro-trace fossils reveal pervasive reworking of Pliocene sapropels by low-oxygen-adapted benthic meiofauna. *Nat. Commun.* **6**, 6589 (2015).
27. Cullen, D. J. Bioturbation of superficial marine sediments by interstitial meiobenthos. *Nature* **242**, 323–324 (1973).
28. Harvey, T. H. P. & Butterfield, N. J. Exceptionally preserved Cambrian loriciferans and the early animal invasion of the meiobenthos. *Nat. Ecol. Evol.* **1**, 0022 (2017).
29. Han, J., Morris, S. C., Ou, Q., Shu, D. & Huang, H. Meiofaunal deuterostomes from the basal Cambrian of Shaanxi (China). *Nature* **542**, 228–231 (2017).
30. de Alvarenga, C. J. S et al. in *Neoproterozoic–Cambrian Tectonics, Global Change and Evolution: A Focus on Southwestern Gondwana* (eds Gaucher, C., Sial, A. N., Halverson, G. P. & Frimmel, H. E.) 15–28 (Elsevier, Amsterdam, 2009).
31. Gaucher, C., Boggiani, P. C., Sprechmann, P., Sial, A. N. & Fairchild, T. R. Integrated correlation of the Vendian to Cambrian Arroyo del Soldado and Corumba groups (Uruguay and Brazil): palaeogeographic, palaeoclimatic and palaeobiologic implications. *Precambrian Res.* **120**, 241–278 (2003).
32. Bowring, S. A. et al. Geochronologic constraints on the chronostratigraphic framework of the Neoproterozoic Huqf Supergroup, Sultanate of Oman. *Am. J. Sci.* **307**, 1097–1145 (2007).
33. Fillion, D. & Pickerill, R. K. *Ichnology of the Cambrian? to Lower Ordovician Bell Island and Wabana Groups of Eastern Newfoundland, Canada* (Palaeontographica Canadiana No. 7, Canadian Society of Petroleum Geologists, St. John's, 1990).
34. Cai, Y., Hua, H., Xiao, S., Schiffbauer, J. D. & & Li, P. Biostratinomy of the late Ediacaran pyritized Gaojiashan Lagerstätte from southern Shaanxi, South China: importance of event deposits. *Palaios* **25**, 487–506 (2010).
35. LoDuca, S., Bykova, N., Wu, M., Xiao, S. & Zhao, Y. Seaweed morphology and ecology during the great animal diversification events of the early Paleozoic: a tale of two floras. *Geobiology* **15**, 588–616 (2017).
36. Virtasalo, J. J., Löwemark, L., Papunen, H., Kotilainen, A. T. & Whitehouse, M. J. Pyritic and baritic burrows and microbial filaments in postglacial lacustrine clays in the northern Baltic Sea. *J. Geol. Soc.* **167**, 1185–1198 (2010).
37. Schratzberger, M. & Ingels, J. Meiofauna matters: the roles of meiofauna in benthic ecosystems. *J. Exp. Mar. Biol. Ecol.* http://dx.doi.org/10.1016/j.jembe.2017.01.007 (2017).
38. Schieber, J. The role of an organic slime matrix in the formation of pyritized burrow trails and pyrite concretions. *Palaios* **17**, 104–109 (2002).
39. Uchman, A. Eocene flysch trace fossils from the Hecho Group of the Pyrenees, northern Spain. *Beringeria* **28**, 3–41 (2001).
40. Garwood, R. & Dunlop, J. The walking dead: Blender as a tool for paleontologists with a case study on extinct arachnids. *J. Paleontol.* **88**, 735–746 (2014).
41. Powilleit, M., Kitlar, J. & Graf, G. Particle and fluid bioturbation caused by the priapulid worm *Halicryptus spinulosus* (v. Seibold). *Sarsia* **79**, 109–117 (1994).
42. Bromley, R. G. *Trace Fossils: Biology, Taxonomy and Applications* (Routledge, London, 2012).
43. Anderson, D. T. *Embryology and Phylogeny in Annelids and Arthropods* (International Series of Monographs in Pure and Applied Biology Zoology, Elsevier, Oxford, 2013).
44. Collins, A. G., Lipps, J. H. & Valentine, J. W. Modern mucociliary creeping trails and the bodyplans of Neoproterozoic trace-makers. *Paleobiology* **26**, 47–55 (2000).
45. Seilacher A. *Trace Fossil Analysis* (Springer, Heidelberg, 2007).

46. Beron, C. et al. The burrowing behavior of the nematode *Caenorhabditis elegans*: a new assay for the study of neuromuscular disorders. *Genes Brain Behav.* **14**, 357–368 (2015).
47. Baliński, A., Sun, Y. & Dzik, J. Traces of marine nematodes from 470 million years old Early Ordovician rocks in China. *Nematology* **15**, 567–574 (2013).
48. McIlroy, D. & Brasier, M. D. Ichnological evidence for the Cambrian Explosion in the Ediacaran to Cambrian succession of Tanafjord, Finnmark, northern Norway. *Geol. Soc. Spec. Publ.* **448**, 351–369 (2016).
49. Borner, J., Rehm, P., Schill, R. O., Ebersberger, I. & Burmester, T. A transcriptome approach to ecdysozoan phylogeny. *Mol. Phylogenet. Evol.* **80**, 79–87 (2014).
50. Hua, H., Pratt, B. R. & Zhang, L.-Y. Borings in *Cloudina* shells: complex predator–prey dynamics in the terminal Neoproterozoic. *Palaios* **18**, 454–459 (2003).
51. Darroch, S. A. F. et al. Biotic replacement and mass extinction of the Ediacara biota. *Proc. R. Soc. B* **282**, 20151003 (2015).
52. Boggiani, P. C. et al. Chemostratigraphy of the Tamengo Formation (Corumba Group, Brazil): a contribution to the calibration of the Ediacaran carbon-isotope curve. *Precambrian Res.* **182**, 382–401 (2010).
53. Gerstenberger, H. & Haase, G. A highly effective emitter substance for mass spectrometric Pb isotope ratio determinations. *Chem. Geol.* **136**, 309–312 (1997).
54. Condon, D. J., Schoene, B., McLean, N. M., Bowring, S. A. & Parrish, R. R. Metrology and traceability of U–Pb isotope dilution geochronology (EARTHTIME tracer calibration part I). *Geochim. Cosmochim. Acta* **164**, 464–480 (2015).
55. McLean, N., Condon, D. J., Schoene, B. & Bowring, S. A. Evaluating uncertainties in the calibration of isotopic reference materials and multi-element isotopic tracers (EARTHTIME tracer calibration part II). *Geochim. Cosmochim. Acta* **164**, 481–501 (2015).
56. Jaffey, A. H., Flynn, K. F., Glendenin, L. E., Bentley, W. C. & Essling, A. M. Precision measurement of half-lives and specific activities of ^{235}U and ^{238}U. *Phys. Rev.* **C4**, 1889–1906 (1971).
57. Hiess, J., Condon, D. J., McLean, N. & Noble, S. R. ^{238}U/^{235}U systematics in terrestrial uranium-bearing minerals. *Science* **335**, 1610–1614 (2012).
58. Hickman-Lewis, K., Garwood, R. J., Withers, P. J. & Wacey, D. X-ray microtomography as a tool for investigating the petrological context of Precambrian cellular remains. *Geol. Soc. Spec. Publ.* **448**, 33–56 (2016).
59. Sutton, M. D., Garwood, R. J., Siveter, D. J. & Siveter, D. J. SPIERS and VAXML; a software toolkit for tomographic visualisation and a format for virtual specimen interchange. *Palaeontol. Electron.* **15**, 1–14 (2012).
60. Garwood, R. et al. Tomographic reconstruction of neopterous Carboniferous insect nymphs. *PLoS ONE* **7**, e45779 (2012).
61. Schindelin, J., Rueden, C. T., Hiner, M. C. & Eliceiri, K. W. The ImageJ ecosystem: an open platform for biomedical image analysis. *Mol. Reprod. Dev.* **82**, 518–529 (2015).
62. Fraley, C. & Raftery, A. E. MCLUST: software for model-based cluster analysis. *J. Classif.* **16**, 297–306 (1999).
63. Darroch, S. A., Laflamme, M. & Clapham, M. E. Population structure of the oldest known macroscopic communities from Mistaken Point, Newfoundland. *Paleobiology* **39**, 591–608 (2013).
64. Grotzinger, J. P., Bowring, S. A., Saylor, B. Z. & Kaufman, A. J. Biostratigraphic and geochronologic constraints on early animal evolution. *Science* **270**, 598–604 (1995).
65. Grazhdankin, D. Patterns of distribution in the Ediacaran biotas: facies versus biogeography and evolution. *Paleobiology* **30**, 203–221 (2004).
66. Martin, M. W. et al. Age of Neoproterozoic bilatarian body and trace fossils, White Sea, Russia: implications for metazoan evolution. *Science* **288**, 841–845 (2000).
67. Condon, D. J. et al. U–Pb ages from the Neoproterozoic Doushantuo Formation, China. *Science* **308**, 95–98 (2005).
68. Yang, C., Li, X. H., Zhu, M. & Condon, D. SIMS U–Pb zircon geochronological constraints on upper Ediacaran stratigraphic correlations, South China. *Geol. Mag.* 1–15 (2016).
69. Pu, J. P. et al. Dodging snowballs: geochronology of the Gaskiers glaciation and the first appearance of the Ediacaran biota. *Geology* **44**, 955–958 (2016).
70. Noble, S. et al. Age and global context of the Ediacaran fossils of Charnwood Forest, Leicestershire, UK. *Geol. Soc. Am. Bull.* **127**, 250–265 (2015).

Acknowledgements

We acknowledge the support and guidance of our co-author M. Brasier in the early stages of this work, and particularly his invitation for L.A.P. to undertake fieldwork in Brazil in 2012. Field costs for L.A.P. were supported by an undergraduate travel grant from St. Anne's College, University of Oxford. Fieldwork costs for M.D.B. were supported by CNPq-Conselho Nacional Desenvolvimento Científico e Tecnológico- Brazil (Proc. 451245/2012-1). This project was supported by an NERC Isotope Geoscience Facilities Steering Committee grant (project IP-1560-0515). J.M.L., P.C.B., R.T., G.A.C.C., C.Q.C.D. and M.L.A.F.P. were supported by grant numbers 2009/02312-4, 2010/02677-0, 2013/17835-8 and 2016-06114-6, São Paulo Research Foundation (FAPESP), Brazil. A.G.L. and L.A.P. are supported by the Natural Environment Research Council (grant numbers NE/L011409/2 and NE/L501554/1, respectively). R.J.G. is a Scientific Associate at the Natural History Museum, London, and a member of the Interdisciplinary Centre for Ancient Life (UMRI). D.M. recognizes the support of an NSERC discovery grant. We are grateful to L. A. dos Santos Reis (Votorantim Cimentos) for facilitating access to the Laginha Mine. We thank L. Tarhan and S. Darroch for constructive reviews.

Author contributions

L.A.P. found and initially identified the *Multina* specimens in the Guaicurus Formation. P.C.B., A.G.L., C.Q.C.D. and J.M.L. found the *Multina* specimens in Tamengo Formation. All authors collaborated to develop this research project. A.G.L. and D.J.C. secured funding for geochronological dating. L.A.P., D.J.C. and R.J.G. conducted the analyses. P.C.B., R.T., J.M.L., C.Q.C.D., M.L.A.F.P. and G.A.C.C. measured the stratigraphic section and collected samples for dating. L.A.P., D.M., D.J.C. and A.G.L. developed the manuscript, and all the authors were involved in data interpretation and the final redrafting of the manuscript.

Competing interests

The authors declare no competing financial interests.

Additional information

Supplementary information is available for this paper at doi:10.1038/s41559-017-0301-9.

Reprints and permissions information is available at www.nature.com/reprints.

Correspondence and requests for materials should be addressed to L.P.

Publisher's note: Springer Nature remains neutral with regard to jurisdictional claims in published maps and institutional affiliations.